

# Antitumor activity of histone deacetylase inhibitors in non-small cell lung cancer cells: development of a molecular predictive model

Akihiko Miyanaga,<sup>1</sup> Akihiko Gemma,<sup>1</sup> Rintaro Noro,<sup>1</sup> Kiyoko Kataoka,<sup>1</sup> Kuniko Matsuda,<sup>1</sup> Michiya Nara,<sup>1</sup> Tetsuya Okano,<sup>1</sup> Masahiro Seike,<sup>1</sup> Akinobu Yoshimura,<sup>1</sup> Akiko Kawakami,<sup>3</sup> Haruka Uesaka,<sup>2</sup> Hiroki Nakae,<sup>2</sup> and Shoji Kudoh<sup>1</sup>

<sup>1</sup>Department of Internal Medicine, Division of Pulmonary Medicine, Infectious Diseases and Oncology, Nippon Medical School, Tokyo, Japan; <sup>2</sup>MediBIC, Tokyo, Japan and <sup>3</sup>Genetic Lab Co., Ltd., Hokkaido, Japan

## Abstract

To ascertain the potential for histone deacetylase (HDAC) inhibitor-based treatment in non-small cell lung cancer (NSCLC), we analyzed the antitumor effects of trichostatin A (TSA) and suberoylanilide hydroxamic acid (vorinostat) in a panel of 16 NSCLC cell lines via 3-(4,5-dimethylthiazol-2-yl)-2,5-diphenyltetrazolium bromide assay. TSA and vorinostat both displayed strong antitumor activities in 50% of NSCLC cell lines, suggesting the need for the use of predictive markers to select patients receiving this treatment. There was a strong correlation between the responsiveness to TSA and vorinostat ( $P < 0.0001$ ). To identify a molecular model of sensitivity to HDAC inhibitor treatment in NSCLC, we conducted a gene expression profiling study using cDNA arrays on the same set of cell lines and related the cytotoxic activity of TSA to corresponding gene expression pattern using a modified National Cancer Institute program. In addition, pathway analysis was done with Pathway Architect software. We used nine genes, which were identified by gene-drug sensitivity correlation and pathway analysis, to build a support vector machine algorithm model by which sensitive cell lines were distinguished from resistant cell lines. The prediction performance of the support vector machine model was

validated by an additional nine cell lines, resulting in a prediction value of 100% with respect to determining response to TSA and vorinostat. Our results suggested that (a) HDAC inhibitors may be promising anticancer drugs to NSCLC and (b) the nine-gene classifier is useful in predicting drug sensitivity to HDAC inhibitors and may contribute to achieving individualized therapy for NSCLC patients. [Mol Cancer Ther 2008;7(7):1923–30]

## Introduction

Several chemotherapy regimens have proven to be effective (1) and are widely applied to treatment for unresected non-small cell lung cancer (NSCLC) (2). However, at present, the effect of these therapies on improving patient survival remains far from satisfactory (1–3). Recently, new therapeutic strategies targeting specific tumor-related genes in NSCLC have been developed, such as the use of small molecules that inhibit epidermal growth factor receptor tyrosine kinase, which show a dramatic antitumor effect in a proportion of patients (1). It is consequently desirable to find more novel therapeutic agents to target NSCLC.

Histone deacetylase (HDAC) and histone acetylase catalyze deacetylation and acetylation, respectively, of histone in eukaryotes, whose dynamic balance is important for the accurate regulation of gene expression in eukaryotes (4). Imbalance in these key enzymes can bring disorder to proliferation and differentiation in normal cells and then lead to tumor initiation. Various HDAC inhibitors, including suberoylanilide hydroxamic acid (vorinostat), MS-275 (Schering), and trichostatin A (TSA), have been reported to exhibit antitumor activities against hematologic, breast, and bladder malignancies (5–9). Although the antitumor activity of HDAC inhibitors against NSCLC has been indicated previously (10–13), these prior studies have been somewhat limited in relation to the number of cell types examined. Here, we examined the sensitivity of a series of NSCLC cell lines to HDAC inhibitors *in vitro* via the 3-(4,5-dimethylthiazol-2-yl)-2,5-diphenyltetrazolium bromide (MTT) assay. Our study showed that TSA and vorinostat displayed strong antitumor activities in a proportion of NSCLC cell lines.

This result indicates the need for the development of biomarkers to predict response of HDAC inhibitor treatment in NSCLC. HDAC inhibitors have been reported to be highly effective in up-regulating expression of tumor suppressor genes, reducing tumor growth, and inducing programmed cell death. However, it seems to be difficult to list predictive biomarkers of HDAC inhibitors only by the status of tumor suppressors. In this study, we built a support vector machine (SVM) algorithm model, by which sensitive cells were distinguished from resistant cells, using

Received 10/12/07; revised 4/2/08; accepted 4/16/08.

**Grant support:** Grant-in-aid for Cancer Research from the Ministry of Health, Labor and Welfare.

The costs of publication of this article were defrayed in part by the payment of page charges. This article must therefore be hereby marked *advertisement* in accordance with 18 U.S.C. Section 1734 solely to indicate this fact.

**Requests for reprints:** Akihiko Gemma, Department of Internal Medicine, Division of Pulmonary Medicine, Infectious Diseases and Oncology, Nippon Medical School, 1-1-5 Sendagi, Bunkyo-ku, Tokyo 113-8602, Japan. Phone: 81-3-3822-2131; Fax: 81-3-5685-3075. E-mail: agemma@nms.ac.jp

Copyright © 2008 American Association for Cancer Research.

doi:10.1158/1535-7163.MCT-07-2140

biomarkers identified by gene expression-TSA drug sensitivity correlation and pathway analysis. A separate set of cancer cell lines validated the prediction performance of this novel SVM model.

## Materials and Methods

### Cell Lines

We analyzed the expression profiles and sensitivity to HDAC inhibitor treatment of separate two sample sets of human NSCLC cell lines. The training sample set consisted of the following 16 cell lines: PC9, PC7, PC14, A549, LK-2, RERF-LC-KJ, RERF-LC-MS, RERF-LC-AI, PC1, PC3, PC10, ABC-1, EBC-1, LC2/ad, SQ5, and QG56 (set 1). The test set consisted of the following 9 cell lines: Lu65, VMRC-LCD, LCOK, NCI-H1650, NCI-H1975, LCI-sq, LC-1F, NCI-H441, and Calu-6 (Set 2). PC7, PC9, PC14, A549, RERF-LC-KJ, RERF-LC-MS, PC3, ABC-1, LC2/ad, VMRC-LCD, LCOK, NCI-H1650, NCI-H1975, and NCI-H441 are adenocarcinoma cell lines. LK-2, RERF-LC-AI, PC1, PC10, EBC-1, LCI-sq, LC-1F, SQ5, and QG56 are squamous cell carcinoma cell lines. Lu65 is a large-cell carcinoma cell line. Calu-6 is an anaplastic carcinoma cell line. The PC1, PC3, PC6, PC7, PC9, PC10, PC14, and QG56 cell lines were obtained from IBL. The A549, NCI-H1650, NCI-H1975, NCI-H441, and Calu-6 cell lines were obtained from the American Type Culture Collection (14). The Lu65, LCOK, and VMRC-LCD cell lines were provided by Y. Shimosato and T. Terasaki (National Cancer Center Research Institute; ref. 14). The LK-2 cell line was obtained from the Health Science Research Resources Bank. PC1, PC3, and PC10 cell lines were provided by S. Hirohashi (National Cancer Center Research Institute). RERF-LC-KJ, LC2/ad, SQ5, LCI-sq, LC-1F, and RERF-LC-AI cell lines were obtained from the RIKEN Cell Bank. RERF-LC-MS, EBC-1, and ABC-1 cell lines were purchased from the Health Science Research Resources Bank.

### MTT Assay for Drug Activity

Estimation of cytotoxicity in the above-mentioned cell types was mediated by a rapid colorimetric assay for mitochondrial dehydrogenase activity as described previously (15–17). Briefly, cell suspensions (200  $\mu$ L;  $10^5$  cells/mL) were seeded into 96-well microtiter plates (Falcon), and 10  $\mu$ L drug solution was added at various concentrations (0.1–20  $\mu$ mol/L). Following 72-h (37°C) exposure to either TSA (Sigma-Aldrich Japan) or vorinostat (Alexis Biochemicals), RPMI 1640 containing 10% FCS, 20  $\mu$ L MTT solution (5 mg/mL in PBS) was added to each well and incubation was then continued for another 4 h at 37°C. Samples were then subjected to spectrophotometric analysis at 560 nm (Ultraspec 4050; LKB).

### RNA Isolation, cDNA Array Hybridization, and Analysis of Hybridization Signals

Total RNA was isolated from untreated cell line using standard protocols described previously (18–20). We did high-density oligonucleotide array analysis using Affymetrix HG-U133A (22,282 probe sets) expression array (Affymetrix; refs. 16, 20). Total RNA was used to synthesize

double-strand cDNA together with SuperScript II and a T7-oligo(dT) primer. Then, biotinylated cRNA was synthesized from the double-stranded cDNA using the RNA Transcript Labeling kit and was purified and fragmented. The fragmented cRNA was hybridized to the oligonucleotide microarray, which was washed and stained with streptavidin-phycoerythrin. Scanning was done with GeneChip Scanner 3000 (Affymetrix). GeneChip analysis was done based on the Affymetrix GeneChip Manual with GeneChip Operating Software version 1.0 (Affymetrix), and Microarray Database software. For GeneChip analysis, the signal intensity was normalized by using the average of all probe sets. Only present call was used. The transcriptomic data we generated for set 1 was deposited previously in Gene Expression Omnibus (GEO accession no. GSE4127). That for set 2 was also deposited in Gene Expression Omnibus (GEO accession no. GSE10089).

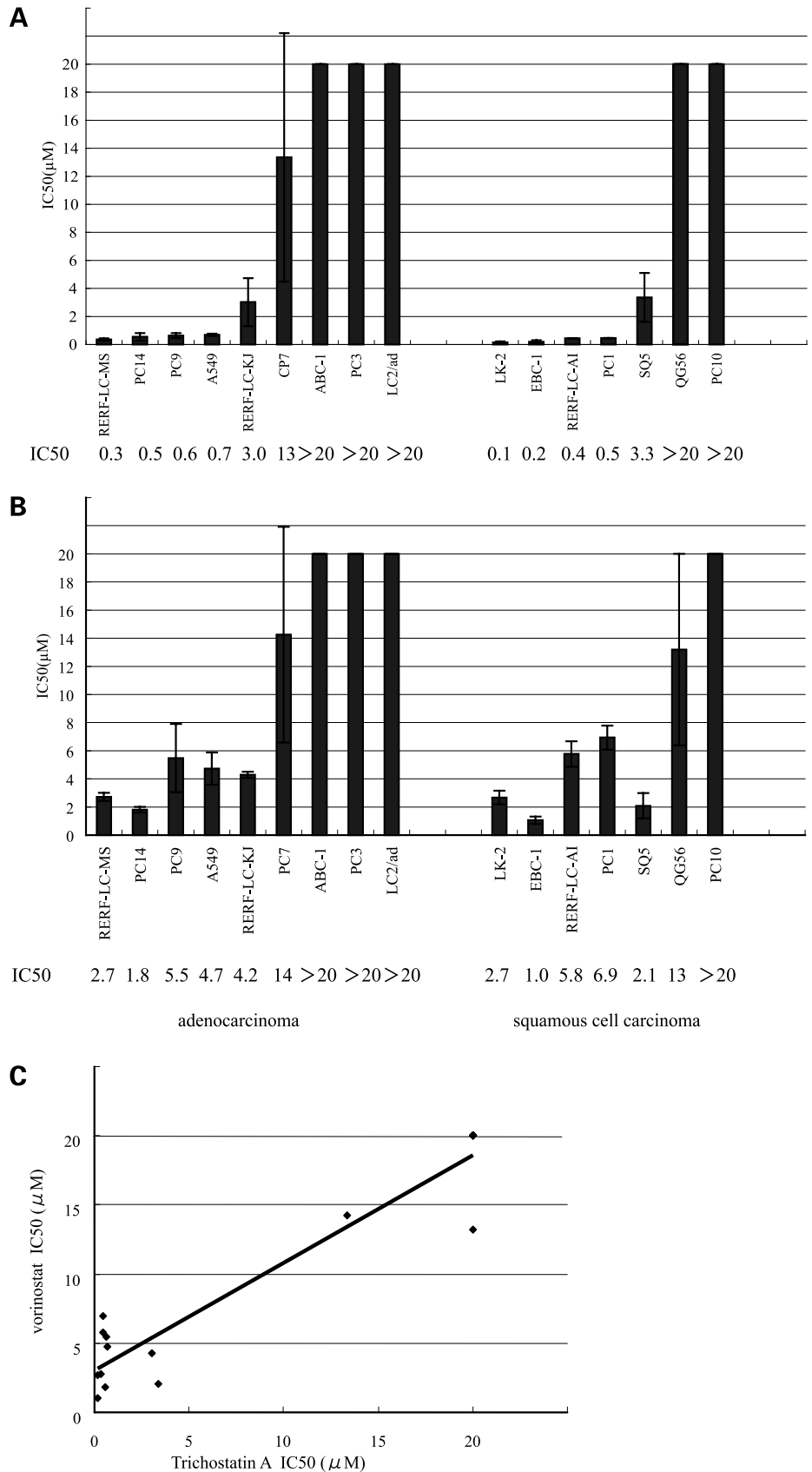
### Data Analysis for Transcriptomic Data

Data analysis for the correlation coefficients that related the drug activity patterns to the expression patterns of the genes was principally done by a modified National Cancer Institute program (CIM-Maker; ref. 21).  $[A]$  ( $IC_{50}$ ) refers to the drug activity matrix in which the rows represent the anticancer drugs and the columns represent the NSCLC cell lines.  $[T]$  (gene expression) refers to the gene expression matrix in which the rows represent individual genes and the columns represent the cell lines. To analyze the relationship between gene expression and drug activity, we generated a gene-drug correlation matrix  $[AT]$  (correlation coefficient) in which the rows represent the genes and the columns represent the drugs. First, we subtracted its mean value from the matrix  $[A]$  in the direction of row and columns for a pretreatment. Secondly, we normalized each element in the matrix  $[A]$  by subtracting its row-wise mean and dividing by its row-wise SD; normalized  $[T]$  was generated in a similar way. Finally, we took the inner product of the matrix  $[A]$  and the transpose of the matrix  $[T]$ . The resulting matrix  $[AT]$  implied the Pearson correlation coefficients that reflected the relationship between drug activity and gene expression.

### Pathway Analysis

We used pathway analysis to provide a viewpoint of the biological function of genes within the proposed classifier. Pathway analysis was done using the Pathway Architect software (Stratagene). All of the known TSA target genes (HDAC1, HDAC2, HDAC3, HDAC4, HDAC5, HDAC6, HDAC7A, HDAC9, and HDAC11) were added to the list of genes identified by gene-drug sensitivity correlation. The pathways showing the relationships among the genes on the list was drawn by selecting all molecules on the pathway edit window. All relationships among the molecules were retrieved from the database, with this information being derived from PubMed abstracts by natural language processing technology. The function was done by selecting the data of maximum reliability (MAX) by choosing all modes of interactions including "Promoter Binding", "Regulation", "Protein Modification", and "Expression" and by taking the relationships supported by

**Figure 1.** **A**, IC<sub>50</sub> values for a panel of 16 NSCLC cell lines responding to TSA treatment as determined via MTT assay. Cell lines were classified as highly sensitive (IC<sub>50</sub> ≤ 1 μmol/L) and resistant (IC<sub>50</sub> > 15 μmol/L) to TSA. **B**, IC<sub>50</sub> values for a panel of 16 NSCLC cell lines responding to vorinostat treatment as determined via MTT assay. Cell lines were classified as highly sensitive (IC<sub>50</sub> ≤ 3 μmol/L) and resistant (IC<sub>50</sub> > 15 μmol/L) to vorinostat. **C**, correlation between the responsiveness to TSA and vorinostat in a panel of 16 NSCLC cell lines (Spearman rank correlation  $r = 0.949$ ,  $P < 0.0001$ ).



Downloaded from <http://aacrjournals.org/mct/article-pdf/7/1/1923/1880899/1923.pdf> by guest on 30 November 2023

three or more consistent data sources. Next, we picked up the incorporated genes out of the imported gene list used at the onset of the pathway analysis, except the subunits of the target gene. Thus, the list of the genes associated with drug response was established in view of not only gene expression profile data but also the biological functions of altered/associated genes. The data from the listed genes were used to build a SVM model with ArrayAssist software (Stratagene) to predict the drug response (IC<sub>50</sub>).

#### Real-time PCR Analysis

Real-time PCR using ABI PRISM 7700 Sequence Detector system (Perkin-Elmer/Applied Biosystems) was done to quantitate the expression of genes associated with HDAC inhibitor response (NQO1, Sec23A, PSME2, MYL6, HNRPD, TM9SF1, PDCD4, and PSMB5). All of the PCR primers and TaqMan fluorogenic probes were obtained from Applied Biosystems. Total RNA was extracted from cultured cells and reverse transcribed using the RevaTra Ace Kit, with a random hexamer being used as primer (Toyobo). A portion of the resulting cDNA was used for quantitative PCR in a 25  $\mu$ L total volume incorporating using the primers, TaqMan probes, and Master Mix, which was composed of PCR buffer, MgCl<sub>2</sub>, dATP, dCTP, dGTP, dUTP, AmpErase UNG, and AmpliTaq Gold DNA polymerase (Perkin-Elmer/Applied Biosystems). The initial thermal cycle conditions were 50°C for 2 min and 95°C for 10 min, as recommended by the manufacturer, followed by 40 cycles of 95°C for 15 s and 60°C for 1 min. Gene expression levels were expressed as ratio of mRNA in a particular sample to the level of glyceraldehyde-3-phos-

phate dehydrogenase mRNA in that sample. Real-time quantitative reverse transcription-PCR was each done in triplicate for each sample (22).

#### Validation Assays

The predictive analysis of the SVM algorithm model was validated by using a separate set of test cell lines. The above-mentioned nine NSCLC cell lines in set 2 were used for this testing process, with the SVM model being applied to classify cell lines as sensitive or resistant based on gene expression profiling data.

## Results

### Effect of HDAC Inhibitors on Cell Growth *In vitro*

Drug sensitivity tests of HDAC inhibitors (TSA and vorinostat) were done on an initial panel of 16 human NSCLC cell lines via MTT analysis. Figure 1 shows the sensitivity of TSA (Fig. 1A) and vorinostat (Fig. 1B) against the training set of cell lines. Accordingly, the concentrations used in the present study are clinically achievable. In our study, TSA and vorinostat both displayed strong antitumor activities in 8 of 16 NSCLC cell lines. There was a strong correlation between the responsiveness to TSA and vorinostat (Spearman rank correlation  $r = 0.949$ ,  $P < 0.0001$ ) in the panel of 16 NSCLC cell lines tested (Fig. 1C). However, the responsiveness to HDAC inhibitors was different from that observed previously with other classes of anticancer agents (16, 17, 20). Clinical trials with vorinostat showed that serum levels in treated patients reached 0.43 to 2.98  $\mu$ mol/L (6, 7). The pharmacokinetic

**Table 1. Factors associated with TSA sensitivity based on expression profiles, sensitivity, and pathway analyses in the 16 NSCLC cell line panel and their functions**

Probe set ID	Gene symbol	Gene title	Genes incorporated by pathway analysis	Correlation coefficients
201064_s_at	PABPC4	Poly(A) binding protein, cytoplasmic 4 (inducible form)		
201737_s_at	MARCH6	Membrane-associated ring finger (C3HC4) 6		
209339_at	SIAH2	Seven in absentia homologue 2 ( <i>Drosophila</i> )		
212887_at	SEC23A	Sec23 homologue A ( <i>Saccharomyces cerevisiae</i> )	+	-0.734
214857_at	C10orf95	Chromosome 10 open reading frame 95		
217100_s_at	UBXD7	UBX domain containing 7		
201762_s_at	PSME2	Proteasome (prosome, macropain) activator subunit 2 (PA28 $\beta$ )	+	-0.683
201919_at	SLC25A36	Solute carrier family 25, member 36		
201993_x_at	HNRPD	Heterogeneous nuclear ribonucleoprotein D like	+	0.678
202731_at	PDCD4	Programmed cell death 4 (neoplastic transformation inhibitor)	+	0.724
208799_at	PSMB5	Proteasome (prosome, macropain) subunit, $\beta$ type, 5	+	-0.688
208912_s_at	CNP	2',3'-cyclic nucleotide 3' phosphodiesterase		
209149_s_at	TM9SF1	Transmembrane 9 superfamily member 1	+	-0.672
209150_s_at	TM9SF1	Transmembrane 9 superfamily member 1	+	-0.672
210519_s_at	NQO1	NAD(P)H dehydrogenase, quinone 1	+	-0.690
211730_s_at	POLR2L	Polymerase (RNA) II (DNA directed) polypeptide L, 7.6-kDa polymerase (RNA) II (DNA directed) polypeptide L, 7.6 kDa		
212082_s_at	MYL6	Myosin, light polypeptide 6, alkali, smooth muscle and nonmuscle	+	-0.718
219717_at	FLJ20280	Hypothetical protein FLJ20280		
220200_s_at	SETD8	SET domain containing (lysine methyltransferase) 8		

analysis of the phase I trial in patients with solid tumor showed that vorinostat was rapidly eliminated and had linear pharmacokinetics with dose-proportional increases in  $C_{max}$  in the dose range of 75 to 900 mg/m<sup>2</sup>. The  $C_{max}$  at 900 mg/m<sup>2</sup> was  $5674 \pm 545$  ng/mL (19.4–23.5  $\mu$ mol/L; ref. 5). In relation to sensitivity to vorinostat, five of these cell lines (RERF-LC-MS, PC14, LK-2, EBC-1, and SQ5) had an  $IC_{50}$  of  $\leq 3$   $\mu$ mol/L (highly-sensitive), four cell lines (PC3, PC10, ABC-1, and LC2/ad) had an  $IC_{50}$  of  $>15$   $\mu$ mol/L (resistant), and the remaining seven cell lines had an  $IC_{50}$  of 3 to 15  $\mu$ mol/L (intermediate sensitive). In the case of TSA, no clinical trials were reported. According to the correlation data (Fig. 1C), cell lines were classified into three groups. Eight of these cell lines (RERF-LC-MS, PC14, PC9, A549, LK-2, EBC-1, RERF-LC-AI, and PC1) had an  $IC_{50}$  of  $\leq 1$   $\mu$ mol/L (highly sensitive), five cell lines (PC3, PC10, ABC-1, LC2/ad, and QG56) had an  $IC_{50}$  of  $>15$   $\mu$ mol/L (resistant), and the remaining three cell lines had an  $IC_{50}$  of 1 to 15  $\mu$ mol/L (intermediate sensitive).

#### Gene Expression-Drug Sensitivity Correlation

We previously used Affymetrix GeneChip technology to perform gene expression profile analysis of the same set of 16 NSCLC cell lines (set 1; ref. 20). To avoid the influence of cell culture artifacts, we separately cultured each cell line in six bottles (22). Signal intensities were normalized by comparison with the average values of all probes. As most of all cell lines belonged to highly sensitive or resistant group in the antitumor sensitivity to TSA, we used the MTT results for TSA for the development of a molecular model of sensitivity to HDAC inhibitors. The top 19 genes associated with TSA sensitivity are listed in Table 1.

#### Pathway Analysis

In addition, pathway analysis was done with Pathway Architect software to provide a viewpoint of the biological function of genes within the proposed classifier. All subunits of the target gene of the compound used in this study (TSA), namely HDAC, were added to Table 1. To try to develop the classifier by the molecules with the biological relation to HDAC, the molecules not incorporated in the drawn pathway in these steps were removed and picked up the incorporated genes out of the imported gene list used at the onset of the pathway analysis, except the subunits of the target gene (Supplementary Fig. S1).<sup>4</sup> Thus, the list of the genes including nine genes associated with the drug response was established in view of not only gene expression profile data but also the biological functions of altered/associated genes (Table 1).

#### Building a SVM Algorithm Model

We used nine genes, which were listed by gene-drug sensitivity correlation and pathway analysis, to build a SVM algorithm model by which eight sensitive cell lines were distinguished from five resistant cell lines (Supple-

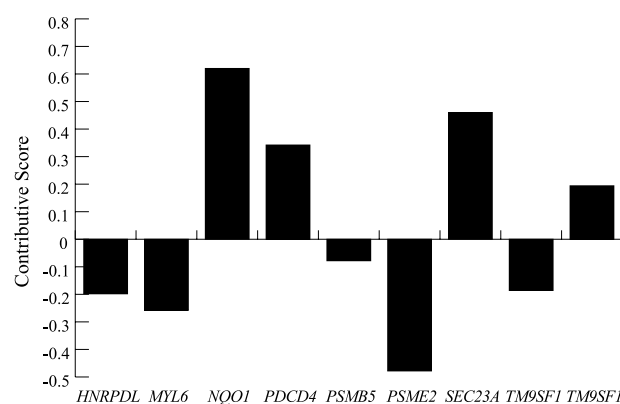


**Figure 2.** Contribution of the nine genes associated with HDAC inhibitor sensitivity. It was calculated based on the independent Partial Least Squares analysis.

mentary Fig. S2A-C).<sup>4</sup> The nine-gene signature was an independent predictor of TSA activity. In this classifier, *PDCD4* and *HNRPDL* were up-regulated and *NQO1*, *SEC23A*, *PSME2*, *MYL6*, *PSMB5*, and *TM9SF1* were down-regulated (Table 1). Of these, three genes (*NQO1*, *SEC23A*, and *PSME2*) were particularly associated with drug activity in Partial Least Squares analysis (Fig. 2).

All training set samples were correctly classified concordant with the preclinical response to TSA treatment (Supplementary Fig. S2A-C).<sup>4</sup> Three cell lines with intermediate sensitivity ( $IC_{50}$ ;  $1 < X < 20$ ) were categorized into the responsive group (Supplementary Fig. S2D).<sup>4</sup> We also validated the prediction performance of this SVM system by testing against an additional nine cell lines, resulting in a prediction value of 100% for determining the response to TSA and vorinostat (Table 2). The nine genes categorized two lines with intermediate sensitivity to TSA treatment into the responsive group. The expression level of these genes, as quantified by GeneChip-based DNA microarray analysis, was validated using real-time PCR (Spearman rank correlation  $r = 0.701$ ,  $P < 0.0001$ ) in the training sample cell lines (Supplementary Table S1).<sup>4</sup>

## Discussion

In our study, HDAC inhibitors displayed strong antitumor activities in 8 of 16 NSCLC cell lines tested, suggesting the need for predictive markers to select patients. With a view toward developing predictive markers for determining response to HDAC inhibitor treatment in the context of individualized therapy for NSCLC, we did a gene expression profiling study using cDNA arrays and related the cytotoxic activity of TSA to corresponding gene expression patterns using a modified National Cancer Institute program. Pathway analysis was also done to reduce substantial false positives based only on the expression level of altered genes. From this analysis, we identified nine genes to build a SVM algorithm model. The

<sup>4</sup> Supplementary material for this article is available at Molecular Cancer Therapeutics Online (<http://mct.aacrjournals.org/>).

**Table 2.** Validation of predictive performance of the nine genes by examining the SVM value in an independent set of nine NSCLC cell lines

	Cell lines	IC <sub>50</sub> (TSA)	IC <sub>50</sub> (vorinostat)	Predicted class	True class (TSA)	True class (vorinostat)
1	LCI-sq	0.19	2.14	Sensitive	Highly sensitive	Highly sensitive
2	VMRC-LCD	0.27	0.87	Sensitive	Highly sensitive	Highly sensitive
3	Lu65	0.34	3.74	Sensitive	Highly sensitive	Intermediate sensitive
4	LCOK	0.52	3.66	Sensitive	Highly sensitive	Intermediate sensitive
5	NCI-H1650	0.89	9.37	Sensitive	Highly sensitive	Intermediate sensitive
6	LC1F	1.26	4.82	Sensitive	Intermediate sensitive	Intermediate sensitive
7	NCI-H1975	1.56	3.96	Sensitive	Intermediate sensitive	Intermediate sensitive
8	NCI-H441	0.77	8.30	Sensitive	Highly sensitive	Intermediate sensitive
9	Calu-6	0.58	2.10	Sensitive	Highly sensitive	Highly sensitive

NOTE: Cell lines were classified as highly sensitive ( $IC_{50} \leq 1 \mu\text{mol/L}$ ), intermediate sensitive ( $1 \mu\text{mol/L} < IC_{50} \leq 15 \mu\text{mol/L}$ ), and resistant ( $IC_{50} > 15 \mu\text{mol/L}$ ) to TSA. In relation to response to vorinostat, cell lines were classified as highly sensitive ( $IC_{50} \leq 3 \mu\text{mol/L}$ ), intermediate sensitive ( $3 \mu\text{mol/L} < IC_{50} \leq 15 \mu\text{mol/L}$ ), and resistant ( $IC_{50} > 15 \mu\text{mol/L}$ ).

prediction performance of the SVM model was validated by an additional nine NSCLC cell lines, resulting in a prediction value of 100% for determining the response to TSA and vorinostat (Table 2).

In previous studies, HDAC inhibitors have been shown to inhibit the proliferation of a wide variety of transformed cells *in vitro*, including lymphoma, myeloma, leukemia, and NSCLC (6), and inhibit tumor growth in rodent models of a variety of solid tumors and hematologic malignancies by both parenteral and oral administration, including prostate cancer (23), leukemia (24), breast cancer (25, 26), glioma (27), and lung cancer (28). In lung cancer, vorinostat and TSA were reported to suppress cell growth of a small number of NSCLC cell lines (12, 29, 30). In our study, these two HDAC inhibitors had distinct and differential activities in the panel of NSCLC cell lines tested. These results suggested that clinical studies in selected NSCLC patients would be required for a more refined evaluation of these drugs.

In this study, nine genes [*NQO1*, *SEC23A*, *PSME2*, *MYL6*, *PSMB5*, *TM9SF1(1)*, *PDCD4*, *HNRPD*, and *TM9SF1(2)*: *TM9SF1(1)* and *TM9SF1(2)* were exons 3 and 6 of the *TM9SF1* gene, respectively] were identified that were associated with the response of HDAC inhibitors in NSCLC cell lines, and three genes (*NQO1*, *SEC23A*, and *PSME2*) were particularly associated with drug activity (Table 1). The *NQO1* gene is a flavoenzyme that catalyzes the two-electron reduction of quinones and nitrogen oxides (31, 32). A major function of this enzyme may be to decrease the formation of reactive oxygen species by decreasing one-electron reductions and associated redox cycling (33). It has been shown to activate some anticancer drugs (34). In addition, it was reported previously that inhibition of *NQO1* reduces the malignant phenotype of pancreatic cancer cells *in vitro* (35). Additionally, another mechanism involved in p53 turnover, apart from the Mdm-2-ubiquitin-proteasome degradation pathway, was regulated by *NQO1* (36). Inhibition of *NQO1* activity by dicoumarol induces p53 and p73 proteasomal degradation, indicating that

*NQO1* plays a role in p53 stabilization (37). Moreover, stress-induced *NQO1* and *NQO2* transiently stabilize p53, which leads to protection against the adverse effects of stressors (38). In addition, interactions of p53 and HDAC were reported to result in p53 deacetylation, thereby reducing its transcriptional activity (39). Therefore, *NQO1* expression may be involved in the activities of HDAC inhibitors.

*PDCD4* is a recently discovered tumor suppressor protein that inhibits protein synthesis by suppression of translation initiation (40). *PDCD4* is ubiquitously expressed in normal tissues, but its expression is lost or suppressed in several tumors, including lung, breast, colon, brain, and prostate cancers (41). Loss of *PDCD4* expression in human lung cancer cells correlates with tumor progression and poor prognosis (42). In addition, ATRA-induced *PDCD4* expression is mediated by inhibition of the phosphatidylinositol 3-kinase/Akt/mTOR survival pathway that constitutively represses *PDCD4* expression in AML cells (43). *PDCD4* was reported to block phosphorylation of c-JUN (44), and inhibition of HDAC may activate mitogen-activated protein kinase pathways such as stress-activated signal transduction pathways by c-Jun NH<sub>2</sub>-terminal kinase leading to AP-1 activation (45). Therefore, *PDCD4* overexpression may influence on the activity of HDAC inhibitors through mitogen-activated protein kinase pathway. Other genes [*SEC23A* (46), *PSME2* (47, 48), *MYL6* (46), *PSMB5* (49), *TM9SF1* (46), and *HNRPD* (49)] have been reported to interact with HDAC signaling in several profiling studies and network analyses. It is unclear how the expression of these genes might be related to the sensitivity of HDAC inhibitors. Otherwise, proteasome subunits, derived from *PSME2* and *PSMB5* genes, are multicatalytic proteinase complexes, which are distributed throughout eukaryotic cells at a high concentration and cleave peptides in an ATP/ubiquitin-dependent process via a nonlysosomal pathway (50). The *SEC23A* and *TM9SF1* genes contribute transporter activity. Other genes were not reported to the associated with drug resistance,

apoptosis, or proliferation. The contributive scores of *TM9SF1* gene were small but on opposite direction. *TM9SF1(1)* and *TM9SF1(2)* are exons 3 and 6, respectively. The transcript variants of this gene were reported.<sup>5</sup>

When using DNA microarray-based gene expression profiling and clinical response data, it is sometimes difficult to consistently reproduce gene-drug sensitivity correlation data. There seem to be several reasons for this difficulty. First, these data are often influenced by sampling methods, sample preservation status, tumor size, tumor environment status including tumor vessels and inflammation, etc. In our study, these influences were minimized due to the use of cultured cell lines. However, cell lines differ from tumors and should therefore be considered as surrogates that may contain information on the molecular cell biology and molecular pharmacology of cancer. Second, the relative list between gene expression and drug activity might contain statistical false positives, in general, even if the precision of the data analysis method is high enough, because all analyses are based only on the expression data originally containing certain dispersion. Here, we used pathway analysis with a view to taking into account the biological function of each gene in an effort to reduce false positives. We showed that the biomarkers listed by gene expression-TSA drug sensitivity correlation and pathway analysis can be confidential if the prediction performance of a SVM model only by these biomarkers was validated.

In conclusion, our results suggested that (a) HDAC inhibitors may be promising anticancer drugs to NSCLC and (b) the nine-gene classifier is useful in predicting drug sensitivity to HDAC inhibitors in NSCLC and may contribute to achieving individualized therapy for NSCLC patients.

## Disclosure of Potential Conflicts of Interest

A. Kawakami: Genetic Lab Co., Ltd., employee. H. Uesaka and H. Nakae: MediBIC employees. The other authors reported no potential conflicts of interest.

## References

- Schiller JH, Harrington D, Belani CP, et al. Eastern Cooperative Oncology Group. Comparison of four chemotherapy regimens for advanced non-small-cell lung cancer. *N Engl J Med* 2002;346:92–8.
- Bonomi P, Kim K, Fairclough D, et al. Comparison of survival and quality of life in advanced non-small-cell lung cancer patients treated with two dose levels of paclitaxel combined with cisplatin versus etoposide with cisplatin: results of an Eastern Cooperative Oncology Group trial. *J Clin Oncol* 2000;18:623–31.
- Shepherd FA, Dancey J, Ramlau R, et al. Prospective randomized trial of docetaxel versus best supportive care in patients with non-small-cell lung cancer previously treated with platinum-based chemotherapy. *J Clin Oncol* 2000;18:2095–103.
- Bi G, Jiang G. The molecular mechanism of HDAC inhibitors in anticancer effects. *Cell Mol Immunol* 2006;3:285–90.
- Kelly WK, Richon VM, O'Connor O, et al. Phase I clinical trial of histone deacetylase inhibitor: suberoylanilide hydroxamic acid administered intravenously. *Clin Cancer Res* 2003;9:3578–88.

6. Kelly WK, O'Connor OA, Krug LM, et al. Phase I study of an oral histone deacetylase inhibitor, suberoylanilide hydroxamic acid, in patients with advanced cancer. *J Clin Oncol* 2005;23:3923–31.

7. Rubin EH, Agrawal NG, Friedman EJ, et al. A study to determine the effects of food and multiple dosing on the pharmacokinetics of vorinostat given orally to patients with advanced cancer. *Clin Cancer Res* 2006;12:7039–45.

8. Duvic M, Talpur R, Ni X, et al. Phase 2 trial of oral vorinostat (suberoylanilide hydroxamic acid, SAHA) for refractory cutaneous T-cell lymphoma (CTCL). *Blood* 2007;109:31–9.

9. Earell JK, Jr., VanOosten RL, Griffith TS. Histone deacetylase inhibitors modulate the sensitivity of tumor necrosis factor-related apoptosis-inducing ligand-resistant bladder tumor cells. *Cancer Res* 2006;66:499–507.

10. Loprevite M, Tiseo M, Grossi F, et al. *In vitro* study of CI-994, a histone deacetylase inhibitor, in non-small cell lung cancer cell lines. *Oncol Res* 2005;15:39–48.

11. Kim HR, Kim EJ, Yang SH, et al. Trichostatin A induces apoptosis in lung cancer cells via simultaneous activation of the death receptor-mediated and mitochondrial pathway? *Exp Mol Med* 2006;38:616–24.

12. Mukhopadhyay NK, Weisberg E, Gilchrist D, et al. Effectiveness of trichostatin A as a potential candidate for anticancer therapy in non-small-cell lung cancer. *Ann Thorac Surg* 2006;81:1034–42.

13. Gore L, Holden SN, Basche M, et al. Updated results from a phase I trial of the histone deacetylase (HDAC) inhibitor MS-275 in patients with refractory solid tumors. *Proc Am Soc Clin Oncol* 2004;22:3026.

14. Gemma A, Seike M, Seike Y, et al. Somatic mutation of the hBUB1 mitotic checkpoint gene in primary lung cancer. *Genes Chromosomes Cancer* 2000;29:213–8.

15. Kobayashi K, Kudoh S, Takemoto T, et al. *In vitro* investigation of a combination of two drugs, cisplatin and carboplatin, as a function of the area under the c/t curve. *J Cancer Res Clin Oncol* 1995;121:715–20.

16. Kokubo Y, Gemma A, Noro R, et al. Reduction of PTEN protein and loss of epidermal growth factor receptor gene mutation in lung cancer with natural resistance to gefitinib (IRESSA). *Br J Cancer* 2005;92:1711–9.

17. Noro R, Gemma A, Kosaihiira S, et al. Gefitinib (IRESSA) sensitive lung cancer cell lines show phosphorylation of Akt without ligand stimulation. *BMC Cancer* 2006;6:277.

18. Gemma A, Hagiwara K, Vincent F, et al. hSmad5 gene, a human hSmad family member: its full length cDNA, genomic structure, promoter region and mutation analysis in human tumors. *Oncogene* 1998;16:951–6.

19. Gemma A, Takenoshita S, Hagiwara K, et al. Molecular analysis of the cyclin dependent kinase inhibitor genes p15INK4B/MTS2, p16 INK4/MTS1, p18 and p19 in human cancer cell lines. *Int J Cancer* 1996;68:605–11.

20. Gemma A, Li C, Sugiyama Y, et al. Anticancer drug clustering in lung cancer based on gene expression profiles and sensitivity database. *BMC Cancer* 2006;6:174.

21. Scherf U, Ross DT, Waltham M, et al. A gene expression database for the molecular pharmacology of cancer. *Nat Genet* 2000;24:236–44.

22. Gemma A, Takenaka K, Hosoya Y, et al. Altered expression of several genes in highly metastatic subpopulations of a human pulmonary adenocarcinoma cell line. *Eur J Cancer* 2001;37:1554–61.

23. Butler LM, Agus DB, Scher HI, et al. Suberoylanilide hydroxamic acid, an inhibitor of histone deacetylase, suppresses the growth of prostate cancer cells *in vitro* and *in vivo*. *Cancer Res* 2000;60:5165–70.

24. He LZ, Tolentino T, Grayson P, et al. Histone deacetylase inhibitors induce remission in transgenic models of therapy-resistant acute promyelocytic leukemia. *J Clin Invest* 2001;108:1321–30.

25. Cohen LA, Amin S, Marks PA, Rifkind RA, Desai D, Richon VM. Chemoprevention of carcinogen-induced mammary tumorigenesis by the hybrid polar cytodifferentiation agent, suberanilohydroxamic acid (SAHA). *Anticancer Res* 1999;19:4999–5005.

26. Cohen LA, Marks PA, Rifkind RA, et al. Suberoylanilide hydroxamic acid (SAHA), a histone deacetylase inhibitor, suppresses the growth of carcinogen-induced mammary tumors. *Anticancer Res* 2002;22:1497–504.

27. Eyupoglu IY, Hahnen E, Buslei R, et al. Suberoylanilide hydroxamic acid (SAHA) has potent anti-glioma properties *in vitro*, *ex vivo* and *in vivo*. *J Neurochem* 2005;93:992–9.

28. Desai D, Das A, Cohen L, el-Bayoumy K, Amin S. Chemopreventive

<sup>5</sup> [http://www.ensembl.org/Homo\\_sapiens/exonview?transcript=ENST00000261789;db=core;showall=1](http://www.ensembl.org/Homo_sapiens/exonview?transcript=ENST00000261789;db=core;showall=1)

- efficacy of suberoylanilide hydroxamic acid (SAHA) against 4-(methylnitrosamino)-1-(3-pyridyl)-1-butanone (NNK)-induced lung tumorigenesis in female A/J mice. *Anticancer Res* 2003;23:499–503.
29. Komatsu N, Kawamata N, Takeuchi S, et al. SAHA, a HDAC inhibitor, has profound anti-growth activity against non-small cell lung cancer cells. *Oncol Rep* 2006;15:187–91.
30. Platta CS, Greenblatt DY, kunnimalaiyaan M, Chen H. The HDAC inhibitor trichostatin A inhibits growth of small cell lung cancer cells. *J Surg Res* 2007;142:219–26.
31. Ross D, Siegel D, Beall H, Prakash AS, Mulcahy RT, Gibson NW. DT-diaphorase in activation and detoxification of quinones. *Cancer Metastasis Rev* 1993;12:83–101.
32. Riley RJ, Workman P. DT-diaphorase and cancer chemotherapy. *Biochem Pharmacol* 1992;43:1657–69.
33. Ernster L. DT-diaphorase: a historical review. *Chem Scr* 1987;27A:1–13.
34. Begleiter A, Robotham E, Lacey G, Leith MK. Increased sensitivity of quinone resistant cells to mitomycin C. *Cancer Lett* 1989;45:173–6.
35. Cullen JJ, Hinkhouse MM, Grady M, et al. Dicumarol inhibition of NADPH:quinone oxidoreductase induces growth inhibition of pancreatic cancer via a superoxide-mediated mechanism. *Cancer Res* 2003;63:5513–20.
36. Asher G, Lotem J, Sachs L, Kahana C, Shaul Y. Mdm-2 and ubiquitin-independent p53 proteasomal degradation regulated by NQO1. *Proc Natl Acad Sci U S A* 2002;99:13125–30.
37. Asher G, Lotem J, Kama R, Sachs L, Shaul Y. NQO1 stabilizes p53 through a distinct pathway. *Proc Natl Acad Sci U S A* 2002;74:3099–3104.
38. Gong X, Kole L, Iskander K, Jaiswal AK. NRH:quinone oxidoreductase 2 and NAD(P)H:quinone oxidoreductase 1 protect tumor suppressor p53 against 20S proteasomal degradation leading to stabilization and activation of p53. *Cancer Res* 2007;67:5380–8.
39. Juan LJ, Shia WJ, Chen MH, et al. Histone deacetylases specifically down-regulate p53-dependent gene activation. *J Biol Chem* 2000;275:20436–43.
40. Cmarik JL, Min H, Hegamyer G, et al. Differentially expressed protein Pdc4 inhibits tumor promoter-induced neoplastic transformation. *Proc Natl Acad Sci U S A* 1999;96:14037–42.
41. Goke R, Barth P, Schmidt A, Samans B, Lankat-Buttgereit B. Programmed cell death protein 4 suppresses CDK1/cdc2 via induction of p21(Waf1/Cip1). *Am J Physiol Cell Physiol* 2004;287:C1541–6.
42. Chen Y, Knosel T, Kristiansen G, et al. Loss of PDCD4 expression in human lung cancer correlates with tumour progression and prognosis. *J Pathol* 2003;200:640–6.
43. Ozpolat B, Akar U, Steiner M, et al. Programmed cell death-4 tumor suppressor protein contributes to retinoic acid-induced terminal granulocytic differentiation of human myeloid leukemia cells. *Mol Cancer Res* 2007;5:95–108.
44. Biotomsky N, Böhm M, Klempnauer KH. Transformation suppressor protein Pdc4 interferes with JNK-mediated phosphorylation of c-Jun and recruitment of the coactivator p300 by c-Jun. *Oncogene* 2004;23:7484–93.
45. Rahman I. Oxidative stress, transcription factors and chromatin remodelling in lung inflammation [review]. *Biochem Pharmacol* 2002;64:935–42.
46. Odom DT, Zizlsperger N, Gordon DB, et al. Control of pancreas and liver gene expression by HNF transcription factors. *Science* 2004;303:1378–81.
47. Barton LF, Runnels HA, Schell TD, et al. Immune defects in 28-kDa proteasome activator  $\gamma$ -deficient mice. *J Immunol* 2004;172:3948–54.
48. Naumovski L, Utz PJ, Bergstrom SK, et al. SUP-HD1: a new Hodgkin's disease-derived cell line with lymphoid features produces interferon- $\gamma$ . *Blood* 1989;74:2733–42.
49. Li Z, Van Calcar S, Qu C, et al. A global transcriptional regulatory role for c-Myc in Burkitt's lymphoma cells. *Proc Natl Acad Sci U S A* 2003;100:8164–9.
50. Almond JB, Cohen GM. The proteasome: a novel target for cancer chemotherapy. *Leukemia* 2002;16:433–43.